Measurements on the production and properties of light hypernuclei at STAR

Yuanjing Ji[1*], for the STAR Collaboration

[1]Lawrence Berkeley National Laboratory

Abstract. The hyperon-nucleon (Y-N) interaction, an important ingredient for the nuclear equation-of-state (EoS), remains poorly constrained. Precise measurements of hypernucei intrinsic properties and production yields in heavy-ion collisions are crucial for the understanding of their production mechanisms and the strength of the Y-N interaction. Thanks to the high statistics data taken from the STAR BES II program, a series of hypernuclei measurements are carried out at low energies. In these proceedings, we present the kinematic and centrality dependence of light hypernuclei production yields and strangeness population factor (S_3, S_4) in Au+Au collisions at $\sqrt{s_{\rm NN}}$ = 3 GeV. We also report the energy dependence of $^{3}_{\Lambda}$H yields and S_3 at mid-rapidity from 3 to 27 GeV Au+Au collisions. Precise measurements of $^{4}_{\Lambda}$He lifetime and $^{3}_{\Lambda}$H branching ratio are also reported. These results are compared with model calculations and physics implications are discussed.

1 Introduction

Hypernuclei are bound systems of nucleons and hyperons. They introduce additional degree of freedom in baryon interactions from hyperons. Thus, hypernuclei are regarded as natural laboratory to investigate hyperon-nucleon (Y-N) interactions. Y-N interaction is the important ingredient for understanding the Equation of State (EoS) of neutron stars and the hadronic phase of heavy-ion collisions. Thermal models [1] predict that hypernuclei are abundantly produced in heavy-ion collisions at high baryon density regions. The second phase of the Beam Energy Scan at RHIC, BES-II program, collects high statistical data in Au+Au collisions with center of mass energies ranging from 3-27 GeV. It maps the QCD phase diagram from 200 MeV baryon chemical potential (μ_B) to around 750 MeV. Thus, BES II program provides us an excellent opportunity to investigate hypernuclei physics in heavy-ion collisions.

2 Analysis details

For low energies collisions (3-17 GeV), the collider can be run under the Fixed-target (FXT) mode to significantly enhance the luminosity. Around 2.6×10^8 good events are collected for 3 GeV Au+Au collisions in 2018. The gold target is located at the west side of the STAR detector, while the gold beam comes from the west to east direction. Tracks are reconstructed by Time Projection Chamber (TPC), which covers the pseudo-rapidity range of $-1.5 < \eta <$

*e-mail: yuanjingji@lbl.gov

0 with respect to the target position. Charged particles are identified utilizing the particle energy loss information provided by TPC. In these proceedings, $^{3}_{\Lambda}$H is reconstructed via both $^{3}_{\Lambda}\mathrm{H} \rightarrow d p \pi^-$ and $^{3}_{\Lambda}\mathrm{H} \rightarrow {}^{3}\mathrm{He}\pi^-$ channels, and $^{4}_{\Lambda}$H and $^{4}_{\Lambda}$He are reconstructed via $^{4}_{\Lambda}\mathrm{H} \rightarrow {}^{4}\mathrm{He}\pi^-$ and $^{4}_{\Lambda}\mathrm{He} \rightarrow {}^{3}\mathrm{He} p \pi^-$. Hypernuclei candidates are reconstructed utilizing KF Particle package [2] to enhance significance.

3 Results and discussions

3.1 Measurements of hypernuclei lifetimes and branching ratio

The $^{3}_{\Lambda}$H branching ratio R_3 is defined as $R_3 = \frac{B.R.(^{3}_{\Lambda}\mathrm{H} \rightarrow {}^{3}\mathrm{He}\pi^-)}{B.R.(^{3}_{\Lambda}\mathrm{H} \rightarrow d p \pi) + B.R.(^{3}_{\Lambda}\mathrm{H} \rightarrow {}^{3}\mathrm{He}\pi)}$. A recent model calculation [3] predicts that $^{3}_{\Lambda}$H R_3 is sensitive to its binding energy, B_Λ, which is directly connected to Y-N interaction strength. The new measurement on $^{3}_{\Lambda}$H R_3 from STAR is highlighted as the red solid star in Fig. 1 (left) with the updated world average value $R_3 = 0.32 \pm 0.03$ shown as the blue band. Figure 1 (right) is the lifetime of $^{4}_{\Lambda}$He, where the STAR new result is indicated by the red circle. The updated world average value is consistent with the calculation based on isospin rule [4].

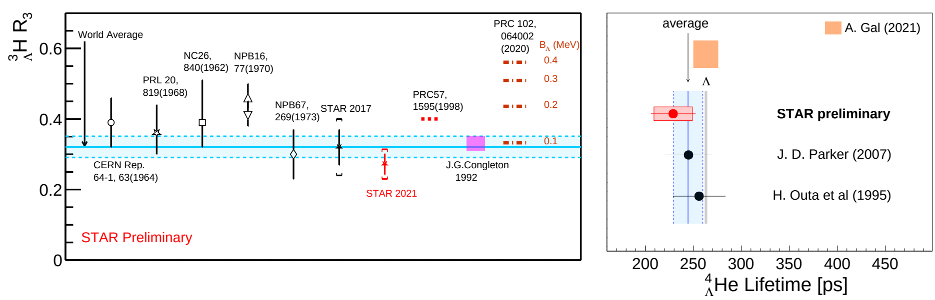

Figure 1. The left plot shows the R_3 of $^{3}_{\Lambda}$H, and the right plot shows the lifetime of $^{4}_{\Lambda}$He. The red solid star (left) and circle (right) markers are the STAR new measurements. The updated world average values are indicated as blue bands.

3.2 Production of hypernuclei in heavy-ion collisions

Figure 2 (left) shows the rapidity dependence of $^{3}_{\Lambda}$H and $^{4}_{\Lambda}$H production yields in Au+Au collisions at 3 GeV [5]. Both $^{3}_{\Lambda}$H and $^{4}_{\Lambda}$H show different trends in 0-10% and 10-50% centralities. Dashed lines are calculations from the transport model (JAM) with instant coalescence of all hadrons as an afterburner [6]. This simple coalescence model can qualitatively describe the data with tuned coalescence parameters. Figure 2 (right) shows the light nuclei and hypernuclei average transverse momentum $\langle p_T \rangle$ as a function of particle mass. A liner trend is observed, suggesting the dominance of collective radial motion. Similar phenomena are also observed in light nuclei and hypernuclei directed flow measurements [7]. Those results are qualitatively consistent with that hypernuclei are produced from the coalescence of hyperons and nucleons.

To investigate the role of Y-N interaction in heavy-ion collisions, we calculate the strangeness population factor [8] that takes Λ baryon over proton yield ratio as a reference to

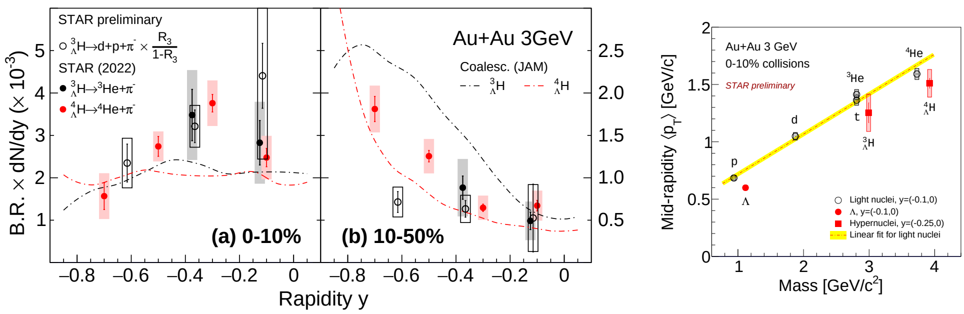

Figure 2. The left plot shows the rapidity dependence of ${}^{3}_{\Lambda}$H (black solid and open circles), ${}^{4}_{\Lambda}$H (red solid circles) $B.R. \times dN/dy$ as a function of rapidity in 0-10% and 10-50% centralities. ${}^{3}_{\Lambda}$H yields via ${}^{3}_{\Lambda}\mathrm{H} \rightarrow dp\pi^{-}$ channel are scaled by a factor of $R_3/(1 - R_3)$. Dashed lines are JAM calculations coupled with instant coalescence [6]. The right plot shows the average transverse momentum $\langle p_T \rangle$ of different particle species as a function of particle mass at mid-rapidity in 3 GeV Au+Au collisions.

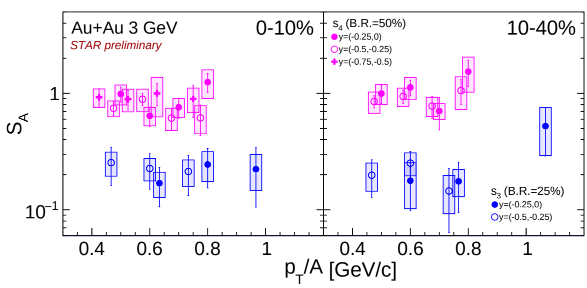

Figure 3. S_3 (blue markers) and S_4 (magenta markers) are shown in as a function of p_T/A, where A is the mass number. S_3 and S_4 are presented in 3 rapidity bins at 0-10% and 10-40% centralities.

hypernuclei to light nuclei yield ratio:

$$S_A = \frac{{}^{A}_{\Lambda}\mathrm{H}(A \times p_T)}{{}^{A}\mathrm{He}(p_T) \times \frac{\Lambda}{p}(p_T)} = \frac{B_A({}^{A}_{\Lambda}\mathrm{H})(p_T)}{B_A({}^{A}\mathrm{He})(p_T)} \tag{1}$$

As one can see in Eq. 1, S_A has a direct connection with the ratio of coalescence parameters B_A. Figure 3 shows $S_A(A = 3, 4)$ as a function p_T/A in 0-10% and 10-40% centralities, where A is the mass number. Within the current uncertainties, no obvious p_T, rapidity and centrality dependence of S_A are observed at 3 GeV. The results imply that B_A of light nuclei and hypernuclei might follow similar tendency versus p_T, rapidity and centralities. Suppressed ${}^{3}_{\Lambda}\mathrm{H}/{}^{3}\mathrm{He}$ yield ratios are observed with respect to Λ/p yield ratio in Au+Au collisions at 3 GeV with $S_3 < 1$. ${}^{4}_{\Lambda}\mathrm{H}/{}^{4}\mathrm{He}$ yield ratio is comparable to Λ/p yield ratio, which can be explained by the feed-down contributions from the exited state ${}^{4}_{\Lambda}\mathrm{H}^{*}(J^{+} = 1)$.

Figure 4 shows the first energy dependence of ${}^{3}_{\Lambda}$H production yields in high μ_B region. An enhanced production of hypernuclei is observed at RHIC BES II energies with respect to LHC energies, which results from the increased baryon density at low energies. The thermal model [1] predicts the trend while can not quantitatively describe the yields. Again, we investigate the strangeness population factor versus collision energy, which removes the absolute difference between Λ and p yields versus beam energy. Figure 5 (right) shows the energy dependence of S_3 from RHIC to LHC energies. A hint of increasing S_3 from $\sqrt{s_{\mathrm{NN}}} =$ 3 GeV to 2.76 TeV is observed. None of the shown models [1, 8, 9] in Fig. 5 (right) can

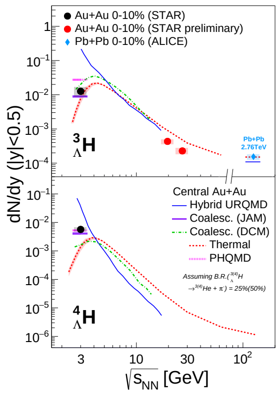

Figure 4. dN/dy of ${}^{3}_{\Lambda}$H (top panel) and ${}^{4}_{\Lambda}$H (bottom panel) at mid-rapidity as a function of the center-of-mass energy. Our results are compared with following model calculations: Hybrid UrQMD [9], JAM [6], DCM [9], Thermal [1], PHQMD[10].

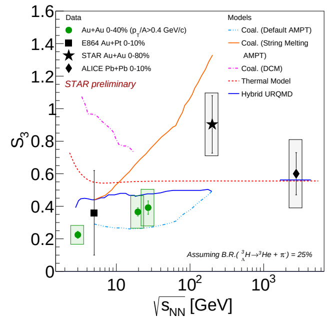

Figure 5. The energy dependence of S_3 is shown. Green circles are the STAR new measurements. Model calculations shown in the plot are from: AMPT [8], DCM [9], Thermal [1], Hybrid UrQMD [9].

describe the S_3 data quantitatively. We are looking forward to further developments from theory communities.

4 Summary

In summary, we present a series of measurements on hypernuclei production and intrinsic properties utilizing high statistics data collected during the BES II program at STAR. We report new measurements on ${}^{4}_{\Lambda}$He lifetime and ${}^{3}_{\Lambda}$H R_3. The kinematic and centrality dependence of ${}^{3}_{\Lambda}$H production yields and S_A in 3 GeV Au+Au collisions are presented. Energy dependence of ${}^{3}_{\Lambda}$H yields and S_A in the mid-rapdity from 3-27 GeV are also reported. Our measurements support the coalescence mechanism of hypernuclei production in heavy-ion collisions. Within the uncertainties, no obvious kinematic or centrality dependence of S_3 is observed in 3 GeV Au+Au collisions. Hopefully, our measurements will set strong constraints on hypernuclei internal structures and inspire new insights into the strength of *Y*-*N* interaction.

References

[1] A. Andronic et al., Phys. Lett. B **697**, 203 (2011), 1010.2995
[2] M. Zyzak, Ph.D. thesis, Frankfurt U. (2016)
[3] F. Hildenbrand, H.W. Hammer, Phys. Rev. C **102**, 064002 (2020), 2007.10122
[4] A. Gal, EPJ Web Conf. **259**, 08002 (2022), 2108.10179
[5] M. Abdallah et al. (STAR), Phys. Rev. Lett. **128**, 202301 (2022), 2110.09513
[6] H. Liu et al., Phys. Lett. B **805**, 135452 (2020), 1909.09304
[7] C. Hu (STAR), EPJ Web Conf. **259**, 11014 (2022)
[8] S. Zhang et al., Phys. Lett. B **684**, 224 (2010), 0908.3357
[9] J. Steinheimer et al., Phys. Lett. B **714**, 85 (2012), 1203.2547
[10] S. Gläßel et al., Phys. Rev. C **105**, 014908 (2022), 2106.14839